Acute doxorubicin cardiotoxicity alters cardiac cytochrome P450 expression and arachidonic acid metabolism in rats

Article *in* Toxicology and Applied Pharmacology · September 2009

DOI: 10.1016/j.taap.2009.09.012 · Source: PubMed

CITATIONS
52

READS
143

4 authors:

Beshay N M Zordoky
University of Minnesota Twin Cities
31 PUBLICATIONS **785** CITATIONS
SEE PROFILE

Anwar Anwar-Mohamed
University of Alberta
49 PUBLICATIONS **588** CITATIONS
SEE PROFILE

Mona E Aboutabl
National Research Center, Egypt
12 PUBLICATIONS **274** CITATIONS
SEE PROFILE

Ayman O S El-Kadi
University of Alberta
176 PUBLICATIONS **3,242** CITATIONS
SEE PROFILE

Toxicology and Applied Pharmacology 242 (2010) 38–46

Contents lists available at ScienceDirect

Toxicology and Applied Pharmacology

journal homepage: www.elsevier.com/locate/ytaap

Acute doxorubicin cardiotoxicity alters cardiac cytochrome P450 expression and arachidonic acid metabolism in rats

Beshay N.M. Zordoky, Anwar Anwar-Mohamed, Mona E. Aboutabl, Ayman O.S. El-Kadi *

Faculty of Pharmacy and Pharmaceutical Sciences, 3126 Dentistry / Pharmacy Centre, University of Alberta, Edmonton, Alberta, Canada T6G 2N8

ARTICLE INFO

Article history:
Received 9 July 2009
Revised 16 September 2009
Accepted 22 September 2009
Available online 29 September 2009

Keywords:
Doxorubicin
Arachidonic acid
Cytochrome P450
Epoxide Hydrolase
Cardiotoxicity

ABSTRACT

Doxorubicin (DOX) is a potent anti-neoplastic antibiotic used to treat a variety of malignancies; however, its use is limited by dose-dependent cardiotoxicity. Moreover, there is a strong correlation between cytochrome P450 (CYP)-mediated arachidonic acid metabolites and the pathogenesis of many cardiovascular diseases. Therefore, in the current study, we have investigated the effect of acute DOX toxicity on the expression of several CYP enzymes and their associated arachidonic acid metabolites in the heart of male Sprague–Dawley rats. Acute DOX toxicity was induced by a single intraperitoneal injection of 15 mg/kg of the drug. Our results showed that DOX treatment for 24 h caused a significant induction of *CYP1A1*, *CYP1B1*, *CYP2C11*, *CYP2J3*, *CYP4A1*, *CYP4A3*, *CYP4F1*, *CYP4F4*, and *EPHX2* gene expression in the heart of DOX-treated rats as compared to the control. Similarly, there was a significant induction of CYP1A1, CYP1B1, CYP2C11, CYP2J3, CYP4A, and sEH proteins after 24 h of DOX administration. In the heart microsomes, acute DOX toxicity significantly increased the formation of 20-HETE which is consistent with the induction of the major CYP ω-hydroxylases: *CYP4A1*, *CYP4A3*, *CYP4F1*, and *CYP4F4*. On the other hand, the formation of 5,6-, 8,9-, 11,12-, and 14,15-epoxyeicosatrienoic acids (EETs) was significantly reduced, whereas the formation of their corresponding dihydroxyeicosatrienoic acids was significantly increased. The decrease in the cardioprotective EETs can be attributed to the increase of sEH activity parallel to the induction of the *EPHX2* gene expression in the heart of DOX-treated rats. In conclusion, acute DOX toxicity alters the expression of several CYP and sEH enzymes with a consequent alteration in arachidonic acid metabolism. These results may represent a novel mechanism by which this drug causes progressive cardiotoxicity.

Introduction

Doxorubicin (DOX, adriamycin) is a potent anthracycline chemotherapeutic agent used to treat a wide variety of human malignancies. However, the clinical use of this highly effective drug is limited by a significant DOX-induced cardiotoxicity which can progress to end-stage heart failure (Christiansen and Autschbach, 2006; Outomuro et al., 2007). The exact mechanism of DOX-induced cardiotoxicity and its progression to heart failure has not been fully elucidated yet; however, several mechanisms have been proposed. These mechanisms include increased oxidative stress, alteration of myocardial energy metabolism, altered molecular signaling, and apoptotic cell death (Nakamura et al., 2000; Ueno et al., 2006; Takemura and Fujiwara, 2007).

We have previously shown that DOX induces the expression of several cytochrome P450 (*CYP*) genes in the cardiac derived H9c2 cells (Zordoky and El-Kadi, 2008a). The importance of CYP enzymes in the cardiovascular physiology emerges from their ability to metabolize arachidonic acid to epoxyeicosatrienoic acids (EETs) and hydroxyeicosatetraenoic acids (HETEs) (Roman, 2002). The cardioprotective effect of EETs has been demonstrated in ischemia–reperfusion injury (Seubert et al., 2007), cardiac hypertrophy (Xu et al., 2006), and recently in DOX-induced cardiotoxicity (Zhang et al., 2009). On the other hand, 20-HETE is known to have a detrimental effect in many cardiovascular diseases (Chabova et al., 2007; Lv et al., 2008; Minuz et al., 2008). Therefore, intricate homeostatic mechanisms are needed to keep the balance between these metabolites. Isoproterenol-induced cardiac hypertrophy has been shown to disturb this balance with increased formation of the cardiotoxic 20-HETE and decreased formation of the cardioprotective EETs (Zordoky et al., 2008). Therefore, we hypothesize that DOX-induced cardiotoxicity will cause a similar disturbance to the CYP-mediated arachidonic acid metabolism.

In addition to CYP enzymes, soluble epoxide hydrolase (sEH) is another major player in determining the level of EETs. The cardioprotective EETs are hydrolyzed by sEH to the less biologically active dihydroxyeicosatrienoic acids (DHETs) (Imig et al., 2002). *EPHX2*, the gene encoding sEH, has been found to be a susceptibility factor for heart failure (Monti et al., 2008). In addition, *EPHX2* gene

Abbreviations: DOX, doxorubicin; CYP, cytochrome P450; SD, Sprague–Dawley; EET, epoxyeicosatrienoic acid; DHET, dihydroxyeicosatrienoic acid; HETE, hydroxyeicosatetraenoic acid; sEH, soluble epoxide hydrolase; LDH, lactate dehydrogenase.

* Corresponding author. Fax: +1 780 492 1217.
E-mail address: aelkadi@pharmacy.ualberta.ca (A.O.S. El-Kadi).

0041-008X/$ – see front matter © 2009 Elsevier Inc. All rights reserved.
doi:10.1016/j.taap.2009.09.012

expression has been reported to increase in animal models of angiotensin II- and isoproterenol-induced cardiac hypertrophy (Zordoky et al., 2008; Ai et al., 2009). Moreover, sEH inhibitors have been shown to prevent and/or reverse the development of cardiac hypertrophy in several models (Xu et al., 2006; Loch et al., 2007; Ai et al., 2009).

Therefore, in the current study, we have investigated the effect of acute DOX cardiotoxicity on the expression of several CYP and sEH enzymes in the heart of male Sprague–Dawley (SD) rats. In addition, we investigated the effect of acute DOX cardiotoxicity on the formation of arachidonic acid metabolites to determine whether the changes in CYP and sEH expression have lead to changes in CYP-mediated arachidonic acid metabolites. Our findings show that DOX-induced cardiotoxicity causes induction of several *CYP* and *EPHX2* genes *in vivo* as well as *in vitro*. In addition, our results provide the first evidence that DOX-induced cardiotoxicity is associated with alteration in cardiac CYP-mediated arachidonic acid metabolism.

Materials and methods

Materials. High-Capacity cDNA Reverse Transcription Kit, SYBR Green SuperMix, and 96-well optical reaction plates with optical adhesive films were purchased from Applied Biosystems (Foster City, CA). Real-time PCR primers were synthesized by Integrated DNA Technologies Inc. (San Diego, CA) according to previously published sequences. Dulbecco's modified Eagle's medium (DMEM) base, arachidonic acid, 4-hydroxybenzophenone, and DOX were purchased from Sigma-Aldrich (St. Louis, MO). Amphotericin B was purchased from ICN Biomedicals Canada (Montreal, QC, Canada). Penicillin-streptomycin, L-glutamine, fetal bovine serum, and TRIzol reagent were purchased from Invitrogen (Carlsbad, CA). Arachidonic acid metabolites standards 5,6-EET, 8,9-EET, 11,12-EET, 14,15-EET, 5,6-DHET, 8,9-DHET, 11,12-DHET, 14,15-DHET, and 20-HETE were obtained from Cayman Chemical (Ann Arbor, MI). Reagents used for liquid chromatographic-electron spray ionization-mass spectrometry (LC-ESI-MS) were at HPLC grade. Acetonitrile and water (HPLC grade) were purchased from EM Scientific (Gibbstawn, NJ). CytoTox-ONE kit was purchased from Promega (Madison, WI). Trans-4-[4-(3-Adamantan-1-yl-ureido)-cyclohexyloxy]-benzoic acid (tAUCB) was a generous gift from Dr Bruce Hammock (University of California, Davis, CA). Acrylamide, *N′N′-bis*-methylene-acrylamide, ammonium persulphate, β-mercaptoethanol, glycine, nitrocellulose membrane (0.45 μm), and TEMED were purchased from Bio-Rad Laboratories (Hercules, CA). Chemiluminescence Western blotting detection reagents were purchased from GE Healthcare Life Sciences (Piscataway, NJ). CYP1B1 rabbit polyclonal primary antibody was purchased from BD Gentest (Bedford, MA). Other primary and secondary antibodies were purchased from Santa Cruz Biotechnology, Inc. (Santa Cruz, CA). Other chemicals were purchased from Fisher Scientific Co. (Toronto, ON, Canada).

Animals. All experimental procedures involving animals were approved by the University of Alberta Health Sciences Animal Policy and Welfare Committee. Male SD rats weighing 300–350 g were obtained from Charles River Canada (St. Constant, QC, Canada). Animals were treated intraperitoneally (IP) with a single 15 mg/kg DOX ($n=18$). Weight-matched controls received the same volume of normal saline ($n=18$). Animals were euthanized 6, 12, and 24 h following the injection under isoflurane anesthesia. All animals were allowed free access to food and water throughout the treatment period. The heart was excised, immediately frozen in liquid nitrogen, and stored at −80 °C until analysis.

Determination of lactate dehydrogenase (LDH). LDH was estimated in rat serum by commercially available kit (CytoTox-One kit, Promega). LDH is measured with a 15-min coupled enzymatic assay that results in the conversion of resazurin into florescent resurofin. The fluorescence produced was then recorded with an excitation wavelength of 560 nm and an emission wavelength of 590 nm according to manufacturer's instructions (Promega). The amount of fluorescence produced is proportional to the amount of LDH which was calculated relative to the control.

Cell culture and treatments. H9c2 cells (American Type Culture Collection, Manassas, VA) were maintained in DMEM, without phenol red, supplemented with 0.45% glucose, 0.15% sodium bicarbonate, 0.11% sodium pyruvate, 10% fetal bovine serum, 20 μM L-glutamine, 100 IU/ml penicillin, 10 μg/ml streptomycin, and 25 ng/ml amphotericin B. Cells were grown in 75-cm^2 tissue culture flasks at 37 °C in a 5% CO_2 humidified incubator. For analysis of mRNA, cells were grown at a density of $1–1.5\times10^6$ cells per well in a 6-well tissue culture plate. On 60–80% confluence (2–3 days), appropriate stock solutions of DOX were directly added to the culture media for 2 h then replaced by normal medium for 24 h.

Cytotoxicity of DOX. The effect of DOX on cell viability was determined by measuring the capacity of reducing enzymes present in viable cells to convert 3-[4,5-dimethylthiazol-2-yl]-2,5-diphenyltetrazolium bromide (MTT) to formazan crystals as described previously (Korashy and El-Kadi, 2004). H9c2 cells were treated for 2 h with various concentrations of DOX. After 24 h, the color intensity in each well was measured at wavelength of 550 nm using EL 312e 96-well microplate readers, Bio-Tek Instruments Inc. (Winooski, VT). The percentage of cell viability was calculated relative to control wells designated as 100% viable cells.

RNA extraction and cDNA synthesis. Total RNA from the frozen tissues and from H9c2 cells was isolated using TRIzol reagent (Invitrogen) according to the manufacturer's instructions and quantified by measuring the absorbance at 260 nm. RNA quality was determined by measuring the 260/280 ratio. Thereafter, first-strand cDNA synthesis was performed by using the high-capacity cDNA reverse transcription kit (Applied Biosystems) according to the manufacturer's instructions. Briefly, 1.5 μg of total RNA from each sample was added to a mix of 2.0 μl 10× RT buffer, 0.8 μl 25× dNTP mix (100 mM), 2.0 μl 10× RT random primers, 1.0 μl MultiScribe™ reverse transcriptase, and 3.2 μl nuclease-free water. The final reaction mix was kept at 25 °C for 10 min, heated to 37 °C for 120 min, heated for 85 °C for 5 s, and finally cooled to 4 °C.

Quantification by real-time PCR. Quantitative analysis of specific mRNA expression was performed by real-time PCR, by subjecting the resulting cDNA to PCR amplification using 96-well optical reaction plates in the ABI Prism 7500 System (Applied Biosystems). The 25-μl reaction mix contained 0.1 μl of 10 μM forward primer and 0.1 μl of 10 μM reverse primer (40 nM final concentration of each primer), 12.5 μl of SYBR Green Universal Mastermix, 11.05 μl of nuclease-free water, and 1.25 μl of cDNA sample. The primers used in the current study were chosen from previously published studies (Bleicher et al., 2001; Kalsotra et al., 2002; Wang et al., 2003; Hirasawa et al., 2005; Rollin et al., 2005; Baldwin et al., 2006) and are listed in Table 1. Assay controls were incorporated onto the same plate, namely, no-template controls to test for the contamination of any assay reagents. After sealing the plate with an optical adhesive cover, the thermocycling conditions were initiated at 95 °C for 10 min, followed by 40 PCR cycles of denaturation at 95 °C for 15 s, and annealing/extension at 60 °C for 1 min. Melting curve (dissociation stage) was performed by the end of each cycle to ascertain the specificity of the primers and the purity of the final PCR product.

Real-time PCR data analysis. The real-time PCR data were analyzed using the relative gene expression, i.e. (ΔΔCT) method as described in

Table 1
Primers sequences used for real-time PCR reactions.

Gene	Forward primer	Reverse primer
CYP1A1	CCAAACGAGTTCCGGCCT	TGCCCAAACCAAAGAGAATGA
CYP1B1	GCTTTACTGTGCAAGGGAGACA	GGAAGGAGGATTCAAGTCAGGA
CYP2B1	AACCCTTGATGACCGCAGTAAA	TGTGGTACTCCAATAGGGACAAGATC
CYP2C11	CACCAGCTATCAGTGGATTTGG	GTCTGCCCTTTGCACAGGAA
CYP2E1	AAAGCGTGTGTGTGTTGGAGAA	AGAGACTTCAGGTTAAAATGCTGCA
CYP2J3	CATTGAGCTCACAAGTGGCTTT	CAATTCCTAGGCTGTGATGTCG
CYP4A1	TTGAGCTACTGCCAGATCCCAC	CCCATTTTTGGACTTCAGCACA
CYP4A3	CTC GCC ATA GCC ATG CTT ATC	CCT TCA GCT CAT TCA TGG CAA TC
CYP4F1	CCCCCAAGGCTTTTTGATG	GAGCGCAACGGCAGCT
CYP4F4	CAGGTCTGAAGCAGGTAACTAAGC	CCGTCAGGGTGGCACAGAGT
CYP4F5	AGGATGCCGTGGCTAACTG	GGCTCCAAGCAGCAGAAGA
CYP4F6	TCACTTGACCTTGATGAAGAACAAC	AAGAGAGGTGGATATCACGGAAG
EPHX2	CACATCCAAGCCACCAAGCC	CAGGCCTCCATCCTCCAG
ANP	GGAGCCTGCGAAGGTCAA	TATCTTCGGTACCGGAAGCTGT
BNP	CAGAAGCTGCTGGAGCTGATAAG	TGTAGGGCCTTGGTCCTTTG
B actin	CCAGATCATGTTTGAGACCTTCAA	GTGGTACGACCAGAGGCATACA

Applied Biosystems User Bulletin No.2 and explained further by Livak and Schmittgen (2001). Briefly, the data are presented as the fold change in gene expression normalized to the endogenous reference gene (β-actin) and relative to the untreated control.

Microsomal protein preparation and Western blot analysis. Microsomal protein was prepared from the heart tissue as described previously (Barakat et al., 2001). Briefly, hearts were washed in ice-cold KCl (1.15% w/v), cut into pieces, and homogenized separately in cold sucrose solution (1 g of tissue in 5 ml of 0.25 M sucrose). Microsomal protein from homogenized tissues was separated by differential ultracentrifugation. The final pellet was reconstituted in cold sucrose and stored at −80 °C. Heart microsomal protein concentration was determined by the Lowry method using bovine serum albumin as a standard (Lowry et al., 1951). Western blot analysis was performed using a previously described method (Gharavi and El-Kadi, 2005). Briefly, 20 μg of heart microsomal protein from each treatment group was separated by 10% sodium dodecyl sulfate–polyacrylamide gel (SDS–PAGE) and then electrophoretically transferred to nitrocellulose membrane. Protein blots were then blocked overnight at 4 °C in blocking solution containing 0.15 M sodium chloride, 3 mM potassium chloride, 25 mM Tris-base (TBS), 5% skim milk, 2% bovine serum albumin, and 0.5% Tween-20. After blocking, the blots were incubated with a primary polyclonal mouse anti-rat CYP1A1 antibody for 12 h, or rabbit anti-rat CYP1B1, rabbit anti-rat CYP2C11, rabbit anti-mouse CYP2J, mouse anti-rat CYP4A, and rabbit anti-rat actin for 2 h, or rabbit anti-human sEH for 12 h at 4 °C. Incubation with a peroxidase-conjugated rabbit anti-mouse IgG secondary antibody for CYP1A1, goat anti-rabbit IgG secondary antibody for CYP1B1, CYP2C11, CYP2J, sEH, and actin, or goat anti-mouse IgG secondary antibody for CYP4A was carried out for 2 h at room temperature. The bands were visualized using the enhanced chemiluminescence method according to the manufacturer's instructions (GE Healthcare Life Sciences, Piscataway, NJ). The intensity of the protein bands was quantified, relative to the signals obtained for actin, using ImageJ software (National Institutes of Health, Bethesda, MD, http://rsb.info.nih.gov/ij).

Microsomal incubation and separation of different arachidonic acid metabolites by LC-ESI-MS. Heart microsomes (1 mg protein/mL) were incubated in the incubation buffer (5 mM magnesium chloride hexahydrate dissolved in 0.5 M potassium phosphate buffer pH 7.4) at 37 °C in a shaking water bath (50 rpm). A pre-equilibration period of 5 min was performed. The reaction was initiated by the addition of 1 mM NADPH. Arachidonic acid was added to a final concentration of 50 μM and incubated for 30 min. The reaction was terminated by the addition of 600 μl ice-cold acetonitrile followed by the internal standard, 4-hydroxybenzophenone. Arachidonic acid metabolites were extracted twice by 1 ml ethyl acetate and dried using speed vacuum (Savant, Farmingdale, NY). Extracted arachidonic acid metabolites were analyzed using LC-ESI-MS (Waters Micromass ZQ 4000 spectrometer) method as described previously (Nithipatikom et al., 2001). The mass spectrometer was operated in negative ionization mode with single ion recorder acquisition. The nebulizer gas was obtained from an in house high purity nitrogen source. The temperature of the source was set at 150 °C, and the voltages of the capillary and the cone were 3.51 kV and 25 V, respectively. The samples (10 μl) were separated on reverse phase C18 column (Kromasil, 250×3.2 mm) using linear gradient mobile phase system water/acetonitrile with 0.005% acetic acid as mobile phase at flow rate of 0.2 ml/min. The mobile phase system started at 60% acetonitrile, linearly increased to 80% acetonitrile in 30 min, increased to 100% acetonitrile in 5 min, and held for 5 min. 4-hydroxybenzophenone was used as internal standard.

Statistical analysis. Data are presented as mean ± standard error of the mean (SE). Control and treatment measurements were compared using Student's *t*-test. A one-way analysis of variance (ANOVA) followed by a Student–Newman–Keuls post hoc comparison has been used whenever multiple comparisons are analyzed. A result was considered statistically significant where $p<0.05$.

Results

Effect of DOX treatment on LDH and on the hypertrophic markers

In order to confirm the occurrence of acute cardiotoxicity by DOX treatment, serum LDH was determined. LDH was significantly increased in the serum of DOX-treated rats to about 180% of its control value at 24 h after DOX administration; however, LDH level was not changed at 6 and 12 h after DOX administration (Fig. 1A). In order to investigate the effect of acute DOX cardiotoxicity on the hypertrophic markers, we measured the cardiac gene expression of atrial natriuretic peptide (ANP) and brain natriuretic peptide (BNP) relative to control rats. Our results showed that DOX treatment caused statistically significant inhibition of the hypertrophic markers, ANP, by 40% and 50%, 12 and 24 h after DOX administration, respectively. However, ANP expression was not significantly altered 6 h after DOX administration. On the other hand, there was a time-dependent statistically significant inhibition of BNP by 60%, 70%, and 80% at 6, 12, and 24 h after DOX administration, respectively (Fig. 1B).

Effect of DOX treatment on CYP gene expression

To examine the effect of DOX treatment on the cardiac expression of several *CYP* genes, total RNA was extracted from the heart of both control and DOX-treated rats. Thereafter, the expression of different genes was measured using reverse transcription followed by real-time PCR as described under Materials and methods.

Fig. 2A shows the effect of DOX-induced cardiotoxicity on *CYP1* family gene expression 24 h after DOX administration. DOX treatment caused a significant induction of *CYP1A1* and *CYP1B1* gene expression in the heart by 200% and 330%, respectively. With regard to *CYP2* family, DOX treatment caused a significant induction of the gene expression of two important epoxygenases, *CYP2C11* and *CYP2J3*, by 480% and 180%, respectively, 24 h after DOX administration. However, the gene expression of *CYP2B1* and *CYP2E1* was not significantly altered (Fig. 2B).

With regard to the gene expression of major ω-hydroxylases, Fig. 3 shows the effect of DOX treatment on *CYP4* family gene expression 24 h after DOX administration. Acute DOX cardiotoxicity caused a significant induction of *CYP4A1* and *CYP4A3* by 380% and 300%, respectively (Fig. 3A). Similarly, DOX treatment caused a significant

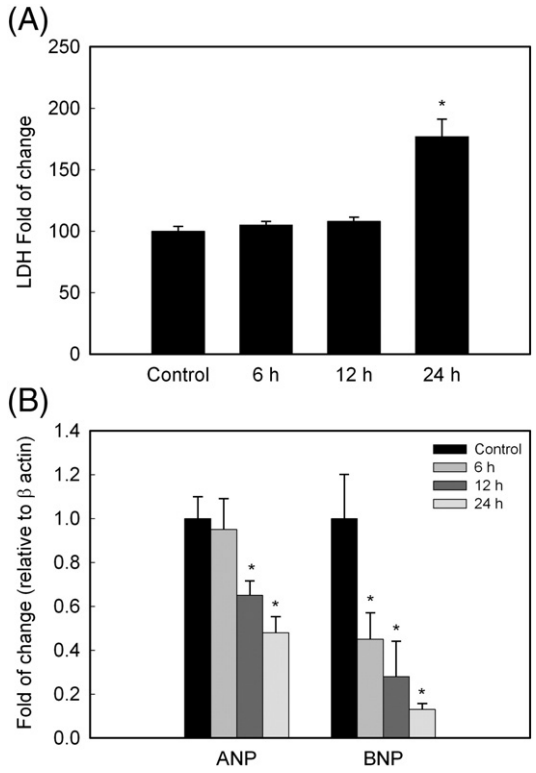

Fig. 1. Effect of acute DOX cardiotoxicity on LDH (A) and on the hypertrophic markers (B). (A) LDH was estimated in the serum by commercially available kit as described under Materials and methods. The amount of LDH was calculated relative to the control and presented as percentage of control and DOX-treated animals for 6, 12, and 24 h. (B) Total RNA was isolated from the hearts of control and DOX-treated animals for 6, 12, and 24 h. ANP and BNP gene expressions were determined by real-time PCR. Results are presented as mean ± SE ($n = 6$). *$p < 0.05$ compared with control.

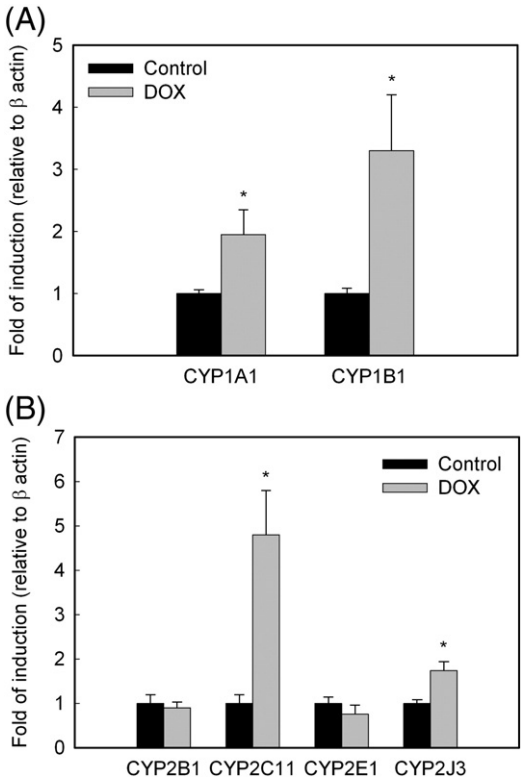

Fig. 2. Effect of acute DOX cardiotoxicity on CYP1 (A) and CYP2 family gene expression (B). Total RNA was isolated from the hearts of control and animals treated with DOX for 24 h. *CYP1A1*, *CYP1B1*, *CYP2B1*, *CYP2C11*, *CYP2E1*, and *CYP2J3* gene expressions were determined by real-time PCR. Results are presented as mean ± SE ($n = 6$). *$p < 0.05$ compared with control.

induction of *CYP4F1* and *CYP4F4* gene expression by 200% and 250%, respectively. However, the expression of *CYP4F5* and *CYP4F6* was not significantly altered (Fig. 3B). Interestingly, all *CYP* gene expression was not significantly altered 6 and 12 h after DOX administration; however, there was a trend of induction of *CYP1A1*, *CYP1B1*, *CYP2C11*, *CYP2J3*, and *CYP4A3* gene expression at 12 h after DOX administration (data not shown).

Effect of DOX treatment on CYP protein expression

To investigate whether the induction of *CYP* gene expression was further translated into functional protein, microsomal protein was prepared from hearts of control and rats treated with DOX for 24 h. Thereafter, CYP1A1, CYP1B1, CYP2C11, CYP2J3, and CYP4A protein levels were determined using Western blot analysis relative to actin as an endogenous control. DOX treatment caused a significant induction of CYP1A1, CYP1B1, CYP2C11, CYP2J3, and CYP4A protein expression by 280%, 345%, 125%, 135%, and 250%, respectively (Fig. 4).

Separation of arachidonic acid metabolites using LC-ESI-MS selected ion chromatogram

LC-ESI-MS has been used in this study for the separation and quantification of CYP-derived metabolites of arachidonic acid. The mass spectrometer was operated in negative ionization mode with single ion recorder acquisition where the most abundant ion is corresponding to the $m/z = [M-1]^-$. All four regioisomeric epoxyeicosatrienoic acids (5,6-, 8,9-, 11,12-, and 14,15-EET) exhibited the most abundant ions corresponding $m/z = 319$ ion, while their corresponding DHETs has $m/z = 337$ ion and 20-HETE has $m/z = 319$ ion. The fact of having functional groups at different positions

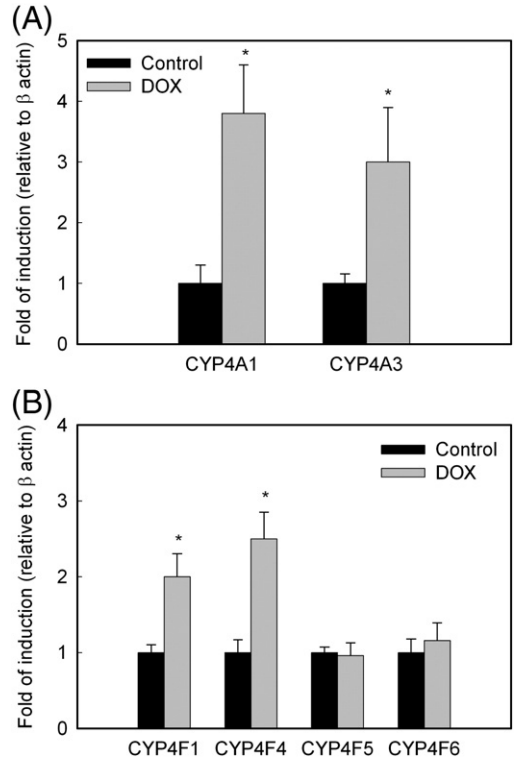

Fig. 3. Effect of acute DOX cardiotoxicity on CYP4A (A) and CYP4F (B) sub-family gene expression. Total RNA was isolated from the hearts of control and animals treated with DOX for 24 h. *CYP4A1*, *CYP4A3*, *CYP4F1*, *CYP4F4*, *CYP4F5* and *CYP4F6* gene expressions were determined by real-time PCR. Results are presented as mean ± SE ($n = 6$). *$p < 0.05$ compared with control.

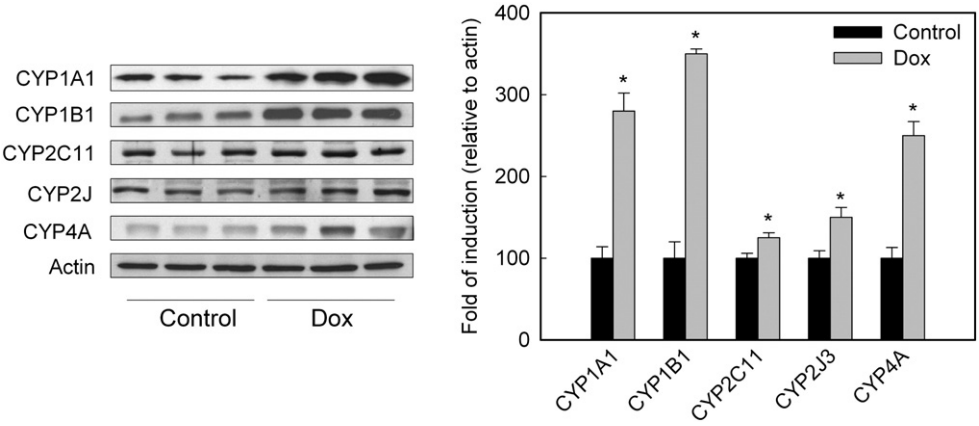

Fig. 4. Effect of acute DOX cardiotoxicity on CYP protein expression. Heart microsomal protein was isolated from the heart of control and animals treated with DOX for 24 h. Twenty micrograms of microsomal protein was separated on a 10% SDS–PAGE. CYP1A1, CYP1B1, CYP2C11, CYP2J, and CYP4A proteins were detected using the enhanced chemiluminescence method. The graph represents the relative amount of CYP protein normalized to the endogenous control (mean ± SE, $n = 3$), and the results are expressed as percentage of the control values taken as 100%. *$p < 0.05$ compared with control.

in the eicosanoids structure allowed successful separation which was achieved through the use of reverse phase C_{18} HPLC column and linear gradient mobile phase. Using authentic standards, 14,15-, 11,12-, 8,9-, and 5,6-EET were found to be eluted at 26.33, 28.56, 29.38, and 30.09 min, respectively, while that of 20-HETE was eluted at 15.07 min. The elution pattern of 14,15-, 11,12-, 8,9-, and 5,6-DHET were at 11.35, 12.58, 13.59, and 14.73 min, respectively.

Effect of DOX treatment on CYP-mediated arachidonic acid metabolism

To investigate the effect of DOX treatment on the formation of CYP-derived arachidonic acid metabolites, heart microsomes of either control or 24 h DOX-treated rats were incubated with 50 μM arachidonic acid for 30 min. Thereafter, arachidonic acid metabolites were determined using LC-ESI-MS. In comparison to control animals, in heart microsomes of DOX-treated rats, the formation of 5,6-, 8,9-, 11,12-, and 14,15-EET were significantly lower by about 60%, 30%, 50%, and 40%, respectively (Fig. 5A). We also measured levels of enzymatic hydration of EETs products, DHETs. As shown in Fig. 5B, the formation of 5,6-, 8,9-, 11,12, and 14,15-DHET was significantly increased by 160%, 200%, 160%, and 150%, respectively, compared to control.

In order to investigate the effect of DOX treatment on the total epoxygenase activity, we calculated the sum of all the products of epoxygenase enzymes, namely the total EETs and DHETs in control and rats treated with DOX for 24 h. The total epoxygenase activity was significantly increased in the heart microsomes of DOX-treated rats by 120% as compared to the control rats (Fig. 6A). On the other hand, to determine the effect of DOX treatment on CYP ω-hydroxylases activity, we determined the formation of 20-HETE in microsomes from control and DOX-treated rats. DOX treatment significantly increased the 20-HETE formation by 190% in comparison to the control group (Fig. 6B).

Effect of DOX treatment on sEH expression and activity

To investigate the mechanism responsible for lower levels of EETs in the heart microsomes of DOX-treated rats despite the increase in the epoxygenase activity, the expression of *EPHX2* gene was determined. Our results show that DOX treatment caused a significant time-dependent induction of *EPHX2* gene expression in the heart by 250%, 300%, and 330% at 6, 12, and 24 h after DOX administration, respectively (Fig. 7A). To confirm the induction of *EPHX2* gene, sEH protein expression was assessed by Western blot analysis. Similar to the induction observed at the mRNA level, sEH protein was significantly induced in the heart microsomes of rats treated with DOX for 24 h by 150% (Fig. 7B).

In addition, sEH activity has been assessed by calculating the ratio of the total DHETs to the total EETs formed in the heart microsomes of control and rats treated with DOX for 24 h. In accordance with the induction at the gene and protein expression levels, sEH activity was induced by 320% in the heart microsomes of rats treated with DOX for

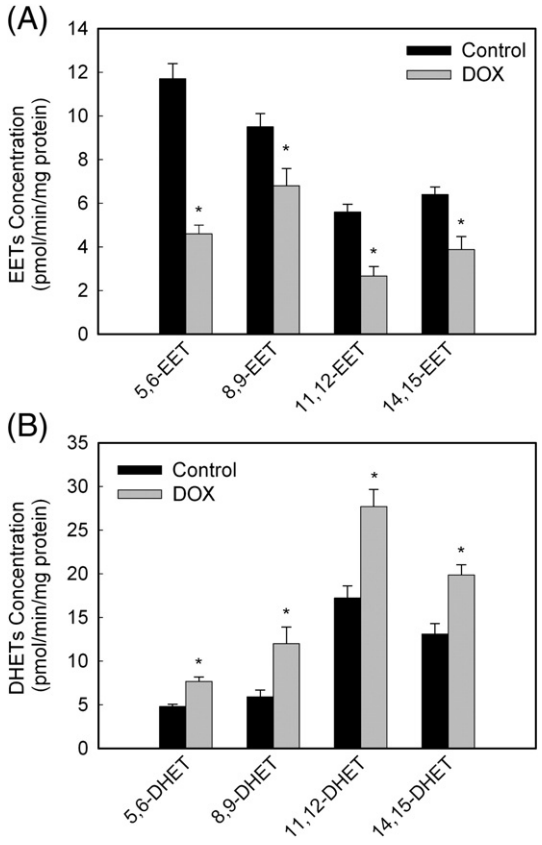

Fig. 5. Effect of acute DOX cardiotoxicity on EETs (A) and DHETs formation (B). Heart microsomes of control or animals treated with DOX for 24 h were incubated with 50 μM arachidonic acid. The reaction was started by the addition of 1 mM NADPH and lasted for 30 min. The reaction was terminated by the addition of ice-cold acetonitrile. EETs and DHETs were extracted twice by 1 ml of ethyl acetate and dried using speed vacuum. Reconstituted metabolites were injected into LC-ESI-MS for metabolite determination. Results are presented as mean ± SE ($n = 6$). *$p < 0.05$ compared with control.

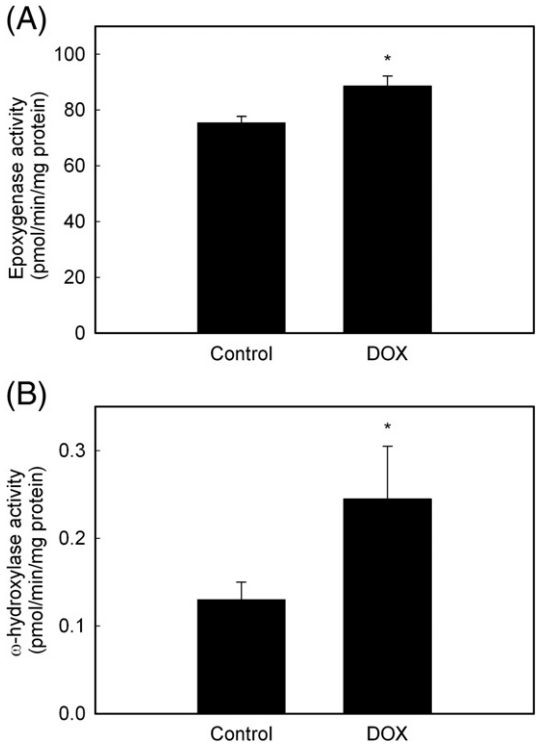

Fig. 6. Effect of acute DOX cardiotoxicity on epoxygenase (A) and ω-hydroxylase activity (B). (A) Epoxygenase activity was determined from the sum of EETs and DHETs formation. (B) ω-hydroxylase activity was determined from the 20-HETE formation. Heart microsomes of control or animals treated with DOX for 24 h were incubated with 50 μM arachidonic acid. The reaction was started by the addition of 1 mM NADPH and lasted for 30 min. The reaction was terminated by the addition of ice-cold acetonitrile. 20-HETE was extracted twice by 1 ml of ethyl acetate and dried using speed vacuum. Reconstituted metabolite was injected into LC-ESI-MS for metabolite determination. Results are presented as mean ± SE ($n = 6$). *$p < 0.05$ compared with control.

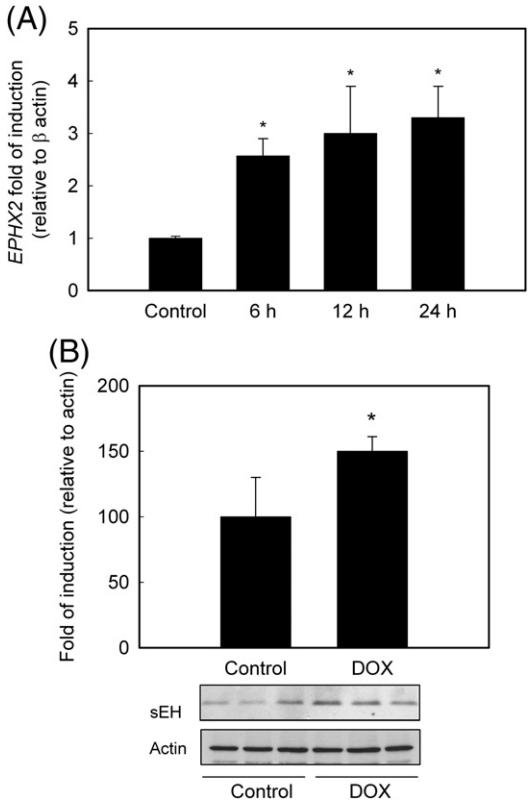

Fig. 7. Effect of acute DOX cardiotoxicity on *EPHX2* gene expression (A) and sEH protein expression (B). (A) Total RNA was isolated from the hearts of control and animals treated with DOX for 6, 12, and 24 h. *EPHX2* gene expression was determined by real-time PCR ($n = 6$). (B) Heart microsomal protein was isolated from the heart of control and animals treated with DOX for 24 h. Twenty micrograms of microsomal protein was separated on a 10% SDS–PAGE. sEH protein was detected using the enhanced chemiluminescence method. The graph represents the relative amount of sEH protein normalized to the endogenous control ($n = 3$). Results are presented as mean ± SE. *$p < 0.05$ compared with control.

24 h (Fig. 8). In order to confirm that the increase in total DHETs/total EETs ratio was due to sEH induction, heart microsomes from control and rats treated with DOX for 24 h were incubated with 100 nM of the selective sEH inhibitor, tAUCB, for 5 min followed by incubation with arachidonic acid as described under Materials and methods. Our results show that inhibition of sEH markedly decreased the total DHETs/total EETs ratio from 1.2 in the control group to 0.3 after incubation with tAUCB. Similarly, the total DHETs/total EETs ratio was decreased from 3.2 in the DOX-treated group to 0.3 after incubation with tAUCB (Fig. 8).

Effect of DOX on the EPHX2 gene expression in H9c2 cells

To investigate whether the induction of *EPHX2* gene expression is due to the direct effect of DOX on the cardiomyocytes, the cardiac derived H9c2 cells were treated with increasing concentrations of DOX. Thereafter, the expression of *EPHX2* was measured using real-time PCR as described under Materials and methods.

To determine the cytotoxic effect of DOX, H9c2 cells were incubated with increasing concentrations of DOX. Thereafter, cell viability was measured by the MTT assay. Our results clearly demonstrate that cells treated with DOX (1–5 μM) maintained more than 90% cell viability (Fig. 9A). Therefore, the observed changes in gene expression are not due to decreased cell viability or toxicity. Our results demonstrated that treatment of H9c2 cells with increasing concentrations of DOX caused a significant concentration-dependent induction of *EPHX2*. The induction was 180%, 210%, and 300% higher than the control with DOX concentrations of 1, 2, and 5 μM, respectively (Fig. 9B).

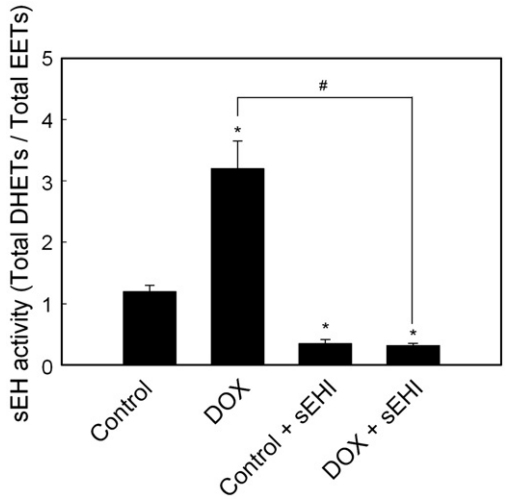

Fig. 8. Effect of acute DOX cardiotoxicity on sEH activity. Heart microsomes of control or animals treated with DOX for 24 h were incubated with 100 nM tAUCB for 5 min followed by incubation with 50 μM arachidonic acid. The reaction was started by the addition of 1 mM NADPH and lasted for 30 min then terminated by the addition of ice-cold acetonitrile. EETs and DHETs were extracted twice by 1 ml of ethyl acetate and dried using speed vacuum. Reconstituted metabolites were injected into LC-ESI-MS for metabolite determination. sEH activity was calculated as the ratio of total DHETs/ total EETs. Results are presented as mean ± SE ($n = 6$). *$p < 0.05$ compared with control, #$p < 0.05$ compared with heart microsomes from animals treated with DOX for 24 h in the absence of sEH inhibitor (sEHI).

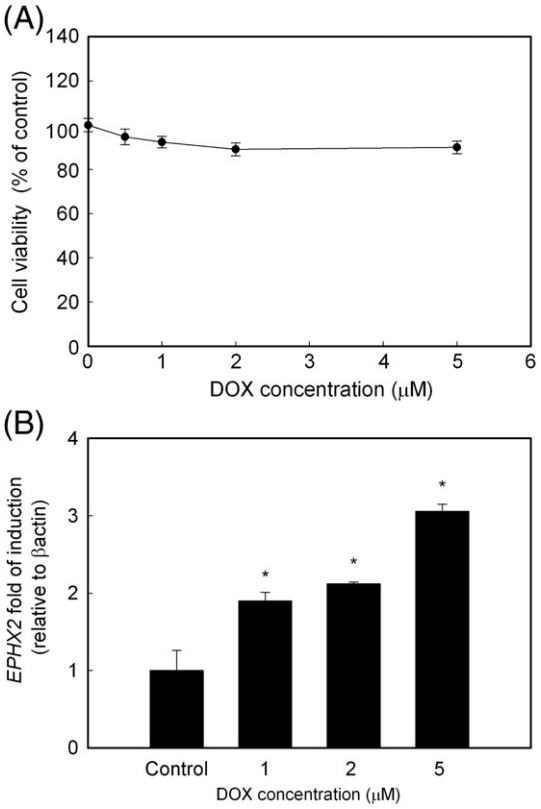

Fig. 9. Effect of DOX on cell viability (A) and *EPHX2* gene expression (B). (A) H9c2 cells were incubated with increasing concentrations of DOX for 2 h and the medium was replaced by fresh medium for another 24 h. Cell viability was measured by the MTT assay as described under Materials and methods. Values are presented as percentage of the control (mean ± SE, $n = 8$). (B) Cells were treated for 2 h with increasing concentrations of DOX (1–5 μM) as described under Materials and methods. Thereafter, total RNA was isolated and the expression of *EPHX2* was determined by real-time PCR. Results are presented as mean ± SE ($n = 6$). *$p < 0.05$ compared with control.

Discussion

We have previously demonstrated that DOX causes a concentration-dependent induction of several *CYP* genes in the cardiac derived H9c2 cells (Zordoky and El-Kadi, 2008a). The physiological importance of CYP enzymes depends on their ability to produce various metabolites that confer cardioprotective or cardiotoxic effects (Zordoky and El-Kadi, 2008b). With regard to their role in arachidonic acid metabolism, CYP enzymes are considered one of the major metabolic pathways for arachidonic acid in addition to the cyclooxygenase and the lipoxygenase pathways. CYP epoxygenases metabolize arachidonic acid to several regioisomers of EETs, while CYP ω-hydroxylases metabolize arachidonic acid to 20-HETE (Roman, 2002). Therefore, the current study demonstrates for the first time the effect of acute DOX cardiotoxicity on cardiac CYP expression and CYP-mediated arachidonic acid metabolism in male SD rats.

In the present study, acute DOX cardiotoxicity has been induced by a single IP injection of 15 mg/kg of DOX. The development of cardiotoxicity has been confirmed by the increased serum LDH level in DOX-treated rats at 24 h after DOX administration. LDH has been used in several studies as a biomarker of cardiotoxicity (Iqbal et al., 2008). In addition, DOX doses between 10 and 20 mg/kg have been widely used to cause acute cardiotoxicity in rats with rapid deterioration of cardiac function, elevation of biomarkers of cardiotoxicity, increased lipid peroxidation, and histopathologic changes (Cigremis et al., 2006; Hydock et al., 2007; Mitra et al., 2007). In addition, our results show that acute DOX cardiotoxicity caused a significant inhibition of the hypertrophic markers, ANP and BNP, with more and earlier inhibition of the BNP than the ANP. In the literature, there is a great discrepancy regarding the effect of DOX on the expression of these markers. In agreement with our results, DOX selectively inhibited BNP versus ANP in cultured neonatal cardiomyocytes (Chen et al., 1999). On the other hand, there was an increase in ANP mRNA in the hearts of DOX-treated dogs and rats; however, *in vitro* DOX treatment significantly decreased ANP gene expression in neonatal cardiomyocytes (Rahman et al., 2001). In H9c2 cells, DOX treatment caused a significant induction of both ANP and BNP (Zordoky and El-Kadi, 2008a). These discrepancies could be attributed to differences in the dose, timing, and the model used.

In the current study, acute DOX cardiotoxicity caused a significant induction of *CYP1A1*, *CYP1B1*, *CYP2C11*, and *CYP2J3* gene expression in the heart of male SD rats 24 h after DOX administration. In addition, there was a significant induction of the protein expression of these enzymes. In agreement with our results, we have recently shown that DOX treatment causes induction of these *CYP* genes in the cardiac derived H9c2 cells after 24 h of exposure to varying DOX concentrations (Zordoky and El-Kadi, 2008a). On the other hand, there was no significant change in the expression of *CYP2B1* and *CYP2E1* genes. In accordance with these results, *CYP2B1* gene expression was not significantly altered by DOX treatment in H9c2 cells; however, *CYP2E1* was significantly induced (Zordoky and El-Kadi, 2008a). Regarding the role of these CYP enzymes in arachidonic acid metabolism, CYP1A1 has been shown to be involved in ω-terminal HETE synthesis, whereas CYP1B1 can metabolize arachidonic acid to both mid-chain HETEs and EETs (Choudhary et al., 2004). CYP2B1, CYP2C11, and CYP2J3 are major epoxygenase enzymes that are involved in arachidonic acid metabolism to EETs (Laethem et al., 1994; Ng et al., 2007), whereas CYP2E1 has been reported to metabolize arachidonic acid to 18- and 19-HETEs (Laethem et al., 1993). In addition, we investigated for the first time the effect of acute DOX cardiotoxicity on the expression of major CYP ω-hydroxylases in the heart of male SD rats. DOX treatment for 24 h caused a significant induction of *CYP4A1*, *CYP4A3*, *CYP4F1*, and *CYP4F4* gene expression, whereas *CYP4F5* and *CYP4F6* expression was not altered. In accordance with the gene expression, there was 200% induction of CYP4A protein in the heart microsomes of rats treated by DOX for 24 h. However, there was no significant change in *CYP* gene expression at 6 and 12 h after DOX administration (data not shown).

To investigate the effect of CYP induction on arachidonic acid metabolism, we performed *in vitro* incubation of heart microsomes with arachidonic acid. We found a significant decrease in 5,6-, 8,9-, 11,12-, and 14,15-EET formation in the heart microsomes of DOX-treated rats compared to the control. This decrease in EETs formation was accompanied by a significant increase in the formation of their corresponding DHETs. In order to estimate the epoxygenase activity, the sum of the total EETs and DHETs was calculated (Zhao et al., 2006). Interestingly, the total epoxygenase activity was significantly higher in the heart microsomes of DOX-treated rats as compared to the control. This increase in the epoxygenase activity can be attributed to the induction of CYP2C11 and CYP2J3, two major CYP epoxygenases, in addition to CYP1B1 which possesses some epoxygenase activity.

Surprisingly, EETs formation is lower in the heart microsomes of DOX-treated rats despite the increase in the epoxygenase activity. Therefore, it was necessary to investigate the effect of acute DOX cardiotoxicity on the expression and activity of sEH which catalyzes the conversion of EETs to DHETs (Imig et al., 2002). In the current study, acute DOX cardiotoxicity caused significant time-dependent induction of the cardiac *EPHX2* gene expression at 6, 12, and 24 h after DOX administration. The induction at the mRNA level was translated to higher sEH protein expression and activity in the heart microsomes of DOX-treated rats in comparison to the control. The increase in sEH activity (3.2-fold) was much higher than the increase in the epoxygenase activity (1.2-fold) which explains the lower level of

EETs despite the increase in epoxygenase activity. To examine whether DOX directly induces *EPHX2* gene expression at the cardiomyocyte level, we used H9c2 cells which is a commercially available myogenic cell line derived from embryonic rat heart ventricles (Kimes and Brandt, 1976). In agreement with the *in vivo* results, DOX treatment caused a significant concentration-dependent induction of *EPHX2 in vitro*.

EETs are reported to have cardioprotective effects through several mechanisms most notably by inhibiting the activation of nuclear factor κB (NF-κB) (Hirotani et al., 2002; Xu et al., 2006). Interestingly, DOX has been shown to induce myocardial apoptosis through activation of NF-κB (Li et al., 2008). Taken together, lower cardiac EETs formation due to sEH induction may be involved in DOX-induced NF-κB activation and the subsequent myocardial apoptosis and cardiotoxicity. In addition, increased oxidative stress has been suggested as one of the main mechanisms of DOX-induced cardiotoxicity (Takemura and Fujiwara, 2007). Taking into account the antioxidant properties of EETs, we can postulate that lower cardiac EETs formation augments DOX-generated oxidative stress and further contributes to its cardiotoxicity. In this context, it has been recently reported that EETs are able to minimize the adverse effects of DOX in the cardiac derived H9c2 cells (Zhang et al., 2009). In addition, sEH inhibitors which prevent EETs degradation thus enhancing their biological activity have been reported to demonstrate a cardioprotective effect in several cardiovascular disease models (Xu et al., 2006; Loch et al., 2007). In the present study, a selective sEH inhibitor, tAUCB, inhibited more than 70% of the conversion of EETs to DHETs in heart microsomes of both control and DOX-treated rats. These results demonstrate that sEH is the major enzyme catalyzing the conversion of EETs to DHETs in rat heart microsomes. In addition, it confirms that the increase in the total DHETs/ total EETs ratio in heart microsomes of DOX-treated rats is due to sEH induction. Therefore, sEH inhibitors may provide a new approach to prevent DOX-induced cardiotoxicity. However, the limitation of this approach is the cancer promoting effect of EETs (Jiang et al., 2007).

With regard to the ω-hydroxylase activity, our results demonstrated that 20-HETE formation is significantly higher in the heart microsomes of rats treated with DOX for 24 h in comparison to untreated animals. The increase in 20-HETE formation in the present work could be attributed to the increased expression of CYP1A1, CYP1B1, CYP4A1, CYP4A3, CYP4F1, and CYP4F4. 20-HETE is known to be involved in many cardiovascular diseases and its formation has been reported to be higher in the hearts of rats with streptozotocin-induced diabetes and isoproterenol-induced cardiac hypertrophy (Zordoky et al., 2008; Yousif et al., 2009). The increase in 20-HETE formation in the microsomes of hypertrophied hearts has been attributed to the induction of *CYP1A1*, *CYP1B1*, and *CYP4A3* gene expression (Zordoky et al., 2008). Interestingly, inhibition of 20-HETE formation caused improvement of the cardiac function following ischemia–reperfusion injury in diabetic rats (Yousif et al., 2009) and reduced cardiomyocyte apoptosis in another model of ischemia–reperfusion injury (Lv et al., 2008). It is important to mention that the induction of CYP enzymes at 24 h following DOX treatment paralleled the initial cardiotoxic effect of DOX which also occurred at 24 h after DOX administration. Therefore, CYP induction can be considered as a result of acute DOX cardiotoxicity. However, induction of ω-hydroxylases and increased 20-HETE formation cannot be ignored as a contributing factor in the progression of acute DOX cardiotoxicity to end-stage heart failure. Taken together, CYP ω-hydroxylase inhibitors may provide another approach to protect against the progression of DOX-induced cardiotoxicity.

In conclusion, DOX-induced cardiotoxicity caused a significant induction of several cardiac CYP and sEH enzymes in male SD rats as well as in the cardiac derived H9c2 cells. The overall effect on arachidonic acid metabolism was a decrease in the cardioprotective EETs and an increase in the cardiotoxic 20-HETE. Induction of sEH may be involved, at least in part, in the development of acute DOX cardiotoxicity. However, CYP induction was a result of acute DOX cardiotoxicity that may be involved in its progression to end-stage heart failure. Therefore, reversal of these changes by increasing the EETs or inhibiting the 20-HETE formation may provide new strategies to protect against the development and/or progression of acute DOX cardiotoxicity.

Conflict of interest statement

The authors declare no conflict of interest.

Acknowledgments

This study was supported by a grant from the Heart and Stroke Foundation of Alberta, NWT, and Nunavut (to A.O.S.E.-K.). B.N.M.Z. and M.E.A. are the recipients of Egyptian Government Scholarships. A. A-M is the recipient of Mike Wolowyk graduate scholarship award. We thank Dr.Vishwa Somayaji for excellent technical assistance with the LC-ESI-MS. We are grateful to Dr. Bruce Hammock for providing us with tAUCB.

References

Ai, D., Pang, W., Li, N., Xu, M., Jones, P.D., Yang, J., Zhang, Y., Chiamvimonvat, N., Shyy, J.Y., Hammock, B.D., Zhu, Y., 2009. Soluble epoxide hydrolase plays an essential role in angiotensin II-induced cardiac hypertrophy. Proc. Natl. Acad. Sci. U. S. A. 106, 564–569.

Baldwin, S.J., Bramhall, J.L., Ashby, C.A., Yue, L., Murdock, P.R., Hood, S.R., Ayrton, A.D., Clarke, S.E., 2006. Cytochrome P450 gene induction in rats ex vivo assessed by quantitative real-time reverse transcriptase-polymerase chain reaction (TaqMan). Drug Metab. Dispos. 34, 1063–1069.

Barakat, M.M., El-Kadi, A.O., du Souich, P., 2001. L-NAME prevents in vivo the inactivation but not the down-regulation of hepatic cytochrome P450 caused by an acute inflammatory reaction. Life Sci. 69, 1559–1571.

Bleicher, K.B., Pippert, T.R., Glaab, W.E., Skopek, T.R., Sina, J.F., Umbenhauer, D.R., 2001. Use of real-time gene-specific polymerase chain reaction to measure RNA expression of three family members of rat cytochrome P450 4A. J. Biochem. Mol. Toxicol. 15, 133–142.

Chabova, V.C., Kramer, H.J., Vaneckova, I., Vernerova, Z., Eis, V., Tesar, V., Skaroupkova, P., Thumova, M., Schejbalova, S., Huskova, Z., Vanourkova, Z., Kolsky, A., Imig, J.D., Cervenka, L., 2007. Effects of chronic cytochrome P-450 inhibition on the course of hypertension and end-organ damage in Ren-2 transgenic rats. Vascul. Pharmacol. 47, 145–159.

Chen, S., Garami, M., Gardner, D.G., 1999. Doxorubicin selectively inhibits brain versus atrial natriuretic peptide gene expression in cultured neonatal rat myocytes. Hypertension 34, 1223–1231.

Choudhary, D., Jansson, I., Stoilov, I., Sarfarazi, M., Schenkman, J.B., 2004. Metabolism of retinoids and arachidonic acid by human and mouse cytochrome P450 1b1. Drug Metab. Dispos. 32, 840–847.

Christiansen, S., Autschbach, R., 2006. Doxorubicin in experimental and clinical heart failure. Eur. J. Cardiothorac. Surg. 30, 611–616.

Cigremis, Y., Parlakpinar, H., Polat, A., Colak, C., Ozturk, F., Sahna, E., Ermis, N., Acet, A., 2006. Beneficial role of aminoguanidine on acute cardiomyopathy related to doxorubicin-treatment. Mol. Cell. Biochem. 285, 149–154.

Gharavi, N., El-Kadi, A.O., 2005. tert-Butylhydroquinone is a novel aryl hydrocarbon receptor ligand. Drug Metab. Dispos. 33, 365–372.

Hirasawa, F., Kawagoe, M., Arany, S., Koizumi, Y., Ueno, Y., Sugiyama, T., 2005. Styrene monomer primarily induces CYP2B1 mRNA in rat liver. Xenobiotica 35, 1089–1099.

Hirotani, S., Otsu, K., Nishida, K., Higuchi, Y., Morita, T., Nakayama, H., Yamaguchi, O., Mano, T., Matsumura, Y., Ueno, H., Tada, M., Hori, M., 2002. Involvement of nuclear factor-kappaB and apoptosis signal-regulating kinase 1 in G-protein-coupled receptor agonist-induced cardiomyocyte hypertrophy. Circulation 105, 509–515.

Hydock, D.S., Lien, C.Y., Schneider, C.M., Hayward, R., 2007. Effects of voluntary wheel running on cardiac function and myosin heavy chain in chemically gonadectomized rats. Am. J. Physiol. Heart Circ. Physiol. 293, H3254–3264.

Imig, J.D., Zhao, X., Capdevila, J.H., Morisseau, C., Hammock, B.D., 2002. Soluble epoxide hydrolase inhibition lowers arterial blood pressure in angiotensin II hypertension. Hypertension 39, 690–694.

Iqbal, M., Dubey, K., Anwer, T., Ashish, A., Pillai, K.K., 2008. Protective effects of telmisartan against acute doxorubicin-induced cardiotoxicity in rats. Pharmacol. Rep. 60, 382–390.

Jiang, J.G., Ning, Y.G., Chen, C., Ma, D., Liu, Z.J., Yang, S., Zhou, J., Xiao, X., Zhang, X.A., Edin, M.L., Card, J.W., Wang, J., Zeldin, D.C., Wang, D.W., 2007. Cytochrome p450 epoxygenase promotes human cancer metastasis. Cancer Res. 67, 6665–6674.

Kalsotra, A., Anakk, S., Boehme, C.L., Strobel, H.W., 2002. Sexual dimorphism and tissue specificity in the expression of CYP4F forms in Sprague Dawley rats. Drug Metab. Dispos. 30, 1022–1028.

Kimes, B.W., Brandt, B.L., 1976. Properties of a clonal muscle cell line from rat heart. Exp. Cell Res. 98, 367–381.

Korashy, H.M., El-Kadi, A.O., 2004. Differential effects of mercury, lead and copper on the constitutive and inducible expression of aryl hydrocarbon receptor (AHR)-regulated genes in cultured hepatoma Hepa 1c1c7 cells. Toxicology 201, 153–172.
Laethem, R.M., Balazy, M., Falck, J.R., Laethem, C.L., Koop, D.R., 1993. Formation of 19(S)-, 19(R)-, and 18(R)-hydroxyeicosatetraenoic acids by alcohol-inducible cytochrome P450 2E1. J. Biol. Chem. 268, 12912–12918.
Laethem, R.M., Halpert, J.R., Koop, D.R., 1994. Epoxidation of arachidonic acid as an active-site probe of cytochrome P-450 2B isoforms. Biochim. Biophys. Acta. 1206, 42–48.
Li, S., EM, Yu, B., 2008. Adriamycin induces myocardium apoptosis through activation of nuclear factor kappaB in rat. Mol. Biol. Rep. 35, 489–494.
Livak, K.J., Schmittgen, T.D., 2001. Analysis of relative gene expression data using real-time quantitative PCR and the 2(-Delta Delta C(T)) method. Methods 25, 402–408.
Loch, D., Hoey, A., Morisseau, C., Hammock, B.O., Brown, L., 2007. Prevention of hypertension in DOCA-salt rats by an inhibitor of soluble epoxide hydrolase. Cell Biochem. Biophys. 47, 87–98.
Lowry, O.H., Rosebrough, N.J., Farr, A.L., Randall, R.J., 1951. Protein measurement with the Folin phenol reagent. J. Biol. Chem. 193, 265–275.
Lv, X., Wan, J., Yang, J., Cheng, H., Li, Y., Ao, Y., Peng, R., 2008. Cytochrome P450 omega-hydroxylase inhibition reduces cardiomyocyte apoptosis via activation of ERK1/2 signaling in rat myocardial ischemia–reperfusion. Eur. J. Pharmacol. 596, 118–126.
Minuz, P., Jiang, H., Fava, C., Turolo, L., Tacconelli, S., Ricci, M., Patrignani, P., Morganti, A., Lechi, A., McGiff, J.C., 2008. Altered release of cytochrome p450 metabolites of arachidonic acid in renovascular disease. Hypertension 51, 1379–1385.
Mitra, M.S., Donthamsetty, S., White, B., Latendresse, J.R., Mehendale, H.M., 2007. Mechanism of protection of moderately diet restricted rats against doxorubicin-induced acute cardiotoxicity. Toxicol. Appl. Pharmacol. 225, 90–101.
Monti, J., Fischer, J., Paskas, S., Heinig, M., Schulz, H., Gosele, C., Heuser, A., Fischer, R., Schmidt, C., Schirdewan, A., Gross, V., Hummel, O., Maatz, H., Patone, G., Saar, K., Vingron, M., Weldon, S.M., Lindpaintner, K., Hammock, B.D., Rohde, K., Dietz, R., Cook, S.A., Schunck, W.H., Luft, F.C., Hubner, N., 2008. Soluble epoxide hydrolase is a susceptibility factor for heart failure in a rat model of human disease. Nat. Genet. 40, 529–537.
Nakamura, T., Ueda, Y., Juan, Y., Katsuda, S., Takahashi, H., Koh, E., 2000. Fas-mediated apoptosis in adriamycin-induced cardiomyopathy in rats: in vivo study. Circulation 102, 572–578.
Ng, V.Y., Huang, Y., Reddy, L.M., Falck, J.R., Lin, E.T., Kroetz, D.L., 2007. Cytochrome P450 eicosanoids are activators of peroxisome proliferator-activated receptor alpha. Drug Metab. Dispos. 35, 1126–1134.
Nithipatikom, K., Grall, A.J., Holmes, B.B., Harder, D.R., Falck, J.R., Campbell, W.B., 2001. Liquid chromatographic-electrospray ionization-mass spectrometric analysis of cytochrome P450 metabolites of arachidonic acid. Anal. Biochem. 298, 327–336.
Outomuro, D., Grana, D.R., Azzato, F., Milei, J., 2007. Adriamycin-induced myocardial toxicity: new solutions for an old problem? Int. J. Cardiol. 117, 6–15.
Rahman, A., Alam, M., Rao, S., Cai, L., Clark, L.T., Shafiq, S., Siddiqui, M.A., 2001. Differential effects of doxorubicin on atrial natriuretic peptide expression in vivo and in vitro. Biol. Res. 34, 195–206.
Rollin, R., Mediero, A., Fernandez-Cruz, A., Fernandez-Durango, R., 2005. Down-regulation of the atrial natriuretic peptide/natriuretic peptide receptor-C system in the early stages of diabetic retinopathy in the rat. Mol. Vis. 11, 216–224.
Roman, R.J., 2002. P-450 metabolites of arachidonic acid in the control of cardiovascular function. Physiol. Rev. 82, 131–185.
Seubert, J.M., Zeldin, D.C., Nithipatikom, K., Gross, G.J., 2007. Role of epoxyeicosatrienoic acids in protecting the myocardium following ischemia/reperfusion injury. Prostaglandins Other Lipid Mediat. 82, 50–59.
Takemura, G., Fujiwara, H., 2007. Doxorubicin-induced cardiomyopathy from the cardiotoxic mechanisms to management. Prog. Cardiovasc. Dis. 49, 330–352.
Ueno, M., Kakinuma, Y., Yuhki, K., Murakoshi, N., Iemitsu, M., Miyauchi, T., Yamaguchi, I., 2006. Doxorubicin induces apoptosis by activation of caspase-3 in cultured cardiomyocytes in vitro and rat cardiac ventricles in vivo. J. Pharmacol. Sci. 101, 151–158.
Wang, S., Hartley, D.P., Ciccotto, S.L., Vincent, S.H., Franklin, R.B., Kim, M.S., 2003. Induction of hepatic phase II drug-metabolizing enzymes by 1,7-phenanthroline in rats is accompanied by induction of MRP3. Drug Metab. Dispos. 31, 773–775.
Xu, D., Li, N., He, Y., Timofeyev, V., Lu, L., Tsai, H.J., Kim, I.H., Tuteja, D., Mateo, R.K., Singapuri, A., Davis, B.B., Low, R., Hammock, B.D., Chiamvimonvat, N., 2006. Prevention and reversal of cardiac hypertrophy by soluble epoxide hydrolase inhibitors. Proc. Natl. Acad. Sci. U. S. A. 103, 18733–18738.
Yousif, M.H., Benter, I.F., Roman, R.J., 2009. Cytochrome P450 metabolites of arachidonic acid play a role in the enhanced cardiac dysfunction in diabetic rats following ischaemic reperfusion injury. Auton. Autacoid. Pharmacol. 29, 33–41.
Zhang, Y., El-Sikhry, H., Chaudhary, K., Batchu, S.N., Shayeganpour, A., Jukar, T.O., Bradbury, J.A., Graves, J.P., Degraff, L.M., Myers, P.H., Rouse, D.C., Foley, J., Nyska, A., Zeldin, D.C., Seubert, J.M., 2009. Overexpression of CYP2J2 provides protection against doxorubicin induced cardiotoxicity. Am. J. Physiol. Heart Circ. Physiol.
Zhao, X., Quigley, J.E., Yuan, J., Wang, M.H., Zhou, Y., Imig, J.D., 2006. PPAR-alpha activator fenofibrate increases renal CYP-derived eicosanoid synthesis and improves endothelial dilator function in obese Zucker rats. Am. J. Physiol. Heart Circ. Physiol. 290, H2187–2195.
Zordoky, B.N., Aboutabl, M.E., El-Kadi, A.O., 2008. Modulation of cytochrome P450 gene expression and arachidonic acid metabolism during isoproterenol-induced cardiac hypertrophy in rats. Drug Metab. Dispos. 36, 2277–2286.
Zordoky, B.N., El-Kadi, A.O., 2008a. Induction of several cytochrome P450 genes by doxorubicin in H9c2 cells. Vascul. Pharmacol. 49, 166–172.
Zordoky, B.N., El-Kadi, A.O., 2008b. Modulation of cardiac and hepatic cytochrome P450 enzymes during heart failure. Curr. Drug Metab. 9, 122–128.